International Journal of Cancer Medicine

Clinical Research | Vol 6 Issue 1

New Automated Quantitative Evaluation of Cancer Cell Proliferation with Ki-67 Method by Unsupervised Learning

Khaled Hammami[1*], Ezzedin Chouat[2], Abdelfattah Zakhama[2], Mohamed Atri[3] and Saber Ben Abdessalem[4]

[1]*Department of Electrical, University of Monastir, Tunisia*

[2]*Department of Medicine, University of Monastir, Tunisia*

[3]*Department of Science, University of Monastir, Tunisia*

[4]*Department of textile-UR Mptex, University of Monastir, Tunisia*

Correspondence should be addressed to Khaled Hammami, Department of Electrical, Engineers School, University of Monastir, Tunisia

Received: September 25, 2022; Accepted: October 06, 2022; Published: October 13, 2022

ABSTRACT

BACKGROUND

Proliferation indexes have a significant impact on the breast tumor's grade and classification and consequently on clinical patient diagnosis. In this article, we propose a novel approach based on computer-assisted analysis of cell images that assists pathologists in the evaluation of Ki-67 index and allow time and effort gain.

METHODS

The procedure is based on the separation and quantification of immunohistochemical stains by the deconvolution of stained images acquired with RGB cameras. It first requires unsupervised learning in the preparation phase to cluster the cells in the ki67 image. Next, mitotic and proliferating cells are labeled using the L*a*b* color space. This space is characterized by a wide homogeneous spectrum of colors close to human perception.

The procedure is based on the separation and the quantification of immunohistochemical staining's by the deconvolution of colored images acquired with RGB cameras. It requires first an unsupervised learning in the preparation phase to reveal cells without debris in the image. Then, mitotic and proliferating cells are labelled using color space L*a*b*. This space is characterized by a broad homogeneous spectrum of colors close to human perception.

RESULT

A good separation was obtained between DAB/Hematoxylin cells with a classification success of 95% and the 96 Ki-67 samples chosen randomly permitted to validate the method.

Citation: Khaled Hammami, New Automated Quantitative Evaluation of Cancer Cell Proliferation with Ki-67 Method by Unsupervised Learning. Int J Can Med 6(1): 46-55.

CONCLUSION

The developed method significantly increased the precision of the calculation of the Ki-67 index. Moreover, our design was evaluated statistically reliable by the unpaired T-test with a confidence coefficient of 95% (n = 96, ρ= 0.13). This represents a great interest for analytical precision and a quite useful decision support tool for pathologists.

KEYWORDS

Immunohistochemistry; Spectral Imaging; Breast cancer; Unsupervised learning; Proliferation index

ABBREVIATION

ACCPRO_IMMUNO	:	Analysis Cancer Cell Proliferation;
BC	:	Breast Cancer;
IHC	:	Immunohistochemistry;
PER	:	Proliferation Evaluate Rate

INTRODUCTION

Immunohistochemistry (IHC) is a method of locating proteins in the cells of a tissue section, by detecting antigens. In fact, an antibody specifically binds to antigens in biological tissues. The IHC staining of estrogen receptors, progesterone (Figure 1) receptors, and the Ki-67 proliferation antigen are widely used in the determination and diagnosis of Breast Cancer (BC). The Ki-67 index can be predicted by radiomic methods using Contrast-Enhanced Computed Tomography (CE-CT) [1]. It is also considered among predictors of the malignant invasion of Nipple-Areolar Complex (NAC) [2].

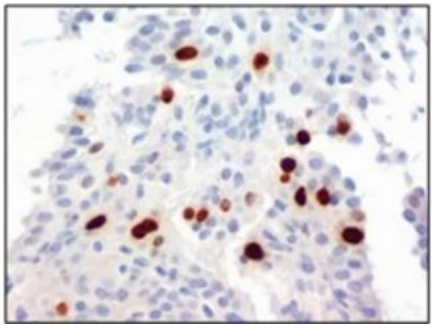

Figure 1: Visualization of nuclear progesterone.

Cell proliferation at the tumour antigen level, as defined by Ki-67 method, is used to define cancerous cell proliferation degree of the patient. Patients with low proliferation tumours are expected to have good treatment results compared to fast-growing tumour patients. The meta-analysis confirmed the role of Ki-67 index as an important prognostic factor for IHC proliferation and a decisive parameter in the classification of BCs and endocrine tumours. It is calculated as the number of positive tumour cells divided by the total number of tumour cells. However, manual calculation of Ki-67 proliferation index leads generally to a variability of inter-observer results [3]. Therefore, Ki-67-based computer algorithm allows automated digital image analysis and consequently accurate calculation of tumour cells can be obtained.

Recent cancer research focus particularly on the extent of inter-observer variability in Ki-67. In fact, the immunoreaction product (brown diaminobenzidine (DAB)) may not accurately reflect the abundance of the Ki-67 antigen [4]. Therefore, systems for discriminating between negatively and positively stained cells have proven useful in research and clinical applications. Proliferation rate estimation (PRE) is an important feature of malignant tumours evaluation and especially in BC [5,6]. The results of the evaluation depend on the large variability of the images and also on the IHC staining procedures [2]. Moreover, PRE method is generally based

on grouping local correlation characteristics and pathological analysis of different cell types and their distribution [7] or by the recognition of cut points and Ki-67 proliferation index calculation [8-28].

Today some automated multispectral image analysis systems like Definiens TissueMap, SlidePath Tissue Image Analysis and InForm software [9,10] or tissue scanning and analysis platforms such as Bacus TMAScore, Dako ACIS III, Genetix Ariol, Aperio Image Analysis, 3DHistech Mirax HistoQuant, Bioimagene Pathiam [10,11] are commercially available. However, these solutions are not always within reach of pathologists. In addition, they require high technical knowledge and good expertise. Therefore, the aim of this paper is to develop an application that solves the problem of the inter-observer variability of Ki-67 and does not require high level of informatics prerequisite from the pathologist.

In the field of research, some works have developed scripts with consumer software such as NIH ImageJ [8,12], or other types of algorithms permitting automatic indexing of images by content. These types of algorithms consider the color as the relevant criterion [13] and the deconvolution is often based on RGB color space [14,15], normalized RGB [8], cyan-magenta-yellow-black (CMYK) [16], HSI [17] or Luv [16]. Some of these methods segment the image into uniform regions [19-21]. However, these methods, despite their importance, face problems of color variation as well as color overlap on the DAB/hematoxylin-stained nuclei and this affects the scan results. Therefore, to improve the analysis procedure, we used in this study the processing in the L*a*b* color space having a broad color spectrum and homogeneous color variations. Moreover, to solve the DAB/Hematoxylin overlap problem, we have integrated a corrective function CF(r).

Furthermore, our contribution aims to facilitate the task of pathologists by using our user-friendly graphic ACCPRO_IMMUNO application developed in C++ language. The application performs images segmentation and provides instantaneously Ki-67 index.

Additionally, our application offers the pathologist the capability to adjust the labelling process in real-time, which allows the analysis results to be further refined.

METHODS

Cell sections are prepared from blocks of formalin-fixed paraffin-embedded tissues in serial slices of 3 µm. After deparaffinization and rehydration, sections are autoclaved at 98°C for 40 minutes in 0.01 M citrate buffer solution (pH 6.0). Endogenous peroxidase is neutralized using 0.5% hydrogen peroxide/methanol for 10 minutes. Sections are incubated at 25°C for 60 minutes with a mouse monoclonal antibody anti-Ki-67 antigen (1:200; MM1; Novocastra, Leica). After washing in Tris-buffered saline (1:10; pH 7.4), the primary antibodies are visualized using secondary biotinylated antibodies, Avidin/Biotin Complex-Horseradish peroxidase with diaminobenzidine (DAB). Finally, sections are counterstained with haematoxylin, dehydrated, cleared and mounted. The human Ki-67 nuclear antigen is expressed in all proliferating cells during the late G1, S, M, and G2 phases of the cell cycle.

Images

A set of 96 images was obtained from sections-stained Ki-67 using a digital camera under an Olympus DP12 microscope. This camera is equipped with a 1/1.8-inch interlaced scanning CCD with a resolution of 3.34 MB. The maximum image resolution is 2048 × 1536 pixels. Images were evaluated twice by 3 pathologists with a wash period of 1 month. Images were stored using a JPG file format. For each imaging session, optimal image brightness and contrast have been adjusted beforehand.

Prognostic Validation

The studied samples come from 96 patients with primary BC. They were carried out in the pathology laboratory at University Hospital of Monastir (Tunisia).

Software Development

Figure 2 shows the diagram of the procedure of automated quantitative analysis of the proliferation of cancerous cells

with pseudo-colors image processing and Ki-67 index calculation.

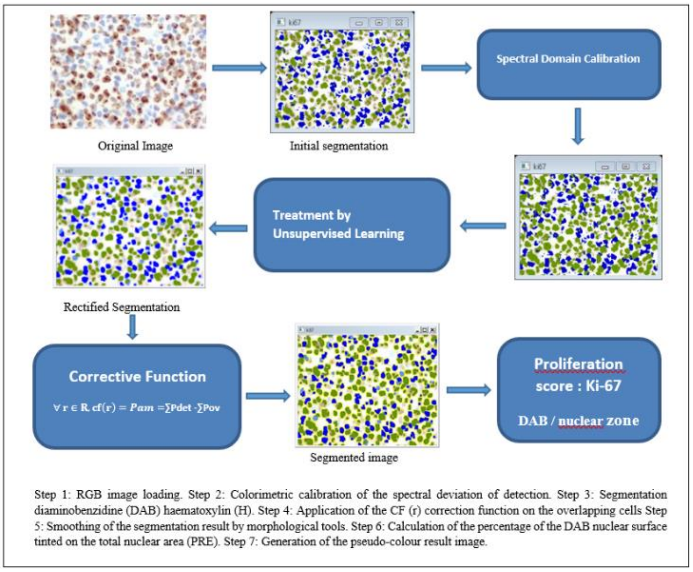

Figure 2: The diagram of the procedure of automated quantitative analysis of the proliferation of cancerous cells.

Treatment

This section corresponds to processing by unsupervised learning.

Treatment by unsupervised learning

The processing is done by K-means, it is an unsupervised non-hierarchical clustering algorithm. It makes it possible to group the similar pixels of the ki67 image into k distinct clusters. A pixel can only be found in one cluster at a time.

Notion of similarity

To be able to group a set of pixels into k distinct clusters, the K-Means algorithm makes it possible to compare the degree of similarity between the different observations. So, two pixels that look alike will have a reduced dissimilarity distance, while two different pixels will have a larger separation distance, see at equation (1).

The Euclidean distance between two pixels is calculated as follows:

$$d(x_1, x_2) = \sqrt{\sum_{j=1}^{n}(x_{1n} - x_{2n})^2} \quad (1)$$

How the K-Means algorithm works

k-means is an iterative algorithm that minimizes the sum of the distances between each individual and the centroid. The initial choice of centroids determines the final result.

Admitting a cloud of a set of points, K-Means changes the points of each cluster until the sum can no longer decrease. The result is a set of compact and clearly separated clusters, subject to choosing the correct value k of the number of clusters.

Algorithmic principal K-means algorithm Hall:

K the number of clusters to form
The pixel matrix

Beginning

Randomly choose K points (a row of the data matrix). These points are the centers of the clusters (called centroid).

Repeat

Assign each point (element of the data matrix) to the group to which it is closest at its center

Recalculate the center of each cluster and modify the centroid.

Until Convergence

OR (stabilization of the total inertia of the population)

End Algorithm

The convergence of the K-Means algorithm is reached when the cluster centers stabilize, i.e., no longer move during the iterations (Figure 3).

Figure 3: Treatment by unsupervised learning.

The Colorimetric Spectrum Detector in the L*a*b* Space

Our algorithm is based on the L*a*b* color space. This space is a color appearance model that models how the human visual system perceives the color of an object taking into account lighting and environment. Several color appearances models have been used by earlier work [7,24]. However, they are considered as primary attempts to quantify color perception. In fact, they are based on the RGB primary system which is not perceptually uniform. Hence, they are not enough efficient in the field of measuring color differences and color prediction.

In this work, we used the CIE-LAB standardized model. It presents the definition of color attributes on a perceptually uniform space that respects the laws of human vision [25]. It allowed managing the changes of illumination by integrating a chromatic adaptation. Hence, it enables to define the distances between the colors.

The colors are identified by three values:

- L, luminance: expressed as a percentage (0 for black to 100 for white).
- a and b: two color ranges from green to red and blue to yellow with values ranging from -120 to +120.

The use of the three RGB components in previous works did not allow reconstituting all the colors perceptible by the human eye. On the other hand, the CIE perceptual models (L*a*b*) are, in fact, based on a scientific analysis of the human perception of color by separating luminance and chrominance parameters. The objective was to develop in a uniform space of colors that is easier to interpret. In L*a*b* models, the calculation of brightness or luminance is made on a basis of the weighting of primary colors (Figure 4). In RGB models the 3 primaries are equivalent.

The equations for colorimetric coordinates are:

$$L^* = 116(Y/Yn)1/3 - 16$$
$$a^* = 500\,[(X/Y)1/3 - (Y/Yn)1/3]$$
$$b^* 200\,[(Y/Yn)1/3 - (Z/Zn)1/3] \quad (2)$$

L*: perceptual lightness.

a* and b*: coordinates of four unique colors of human vision: red, green, blue, and yellow.

Using these equations allows to calculate colorimetric distances on a marked cell according to L, a and b axis.

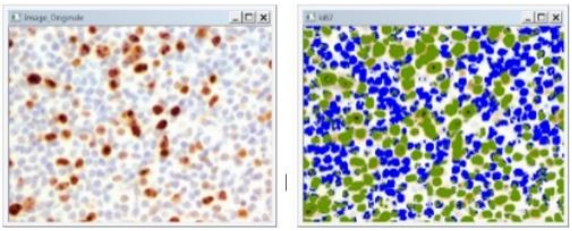

Figure 4: Complete staining by convolution processing based on broad spectrum detection in L*a*b* color space.

Treatment of Color Overlap on Nuclei

At nuclei level, there is an overlap of DAB and hematoxylin (Figure 5). The algorithm allows pixel classification using the color function of the Lab color space and the cell filtering function.

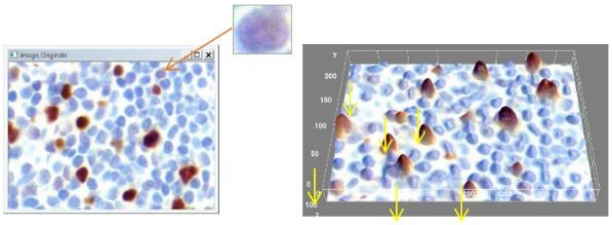

Figure 5: 3D representation for clear visualization of color overlap.

Figure 6 represents 3D visualization of cell with double labelling.

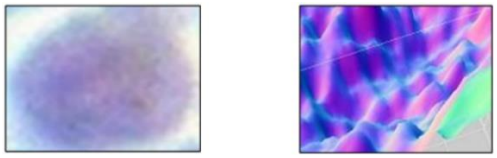

Figure 6: Visualization of 3D overlapping labelling of nuclei.

The separation of proliferated spots from mitotic spots is done by the analysis of their absorption spectra. Figure 7 and Figure 8 show spectral analysis on mitotic cells and double-labelled cells.

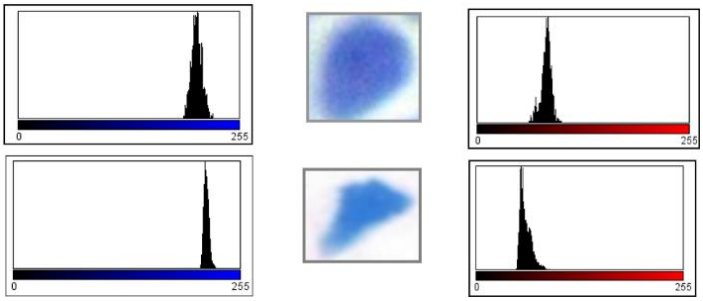

Figure 7: Histogram of mitotic nuclei.

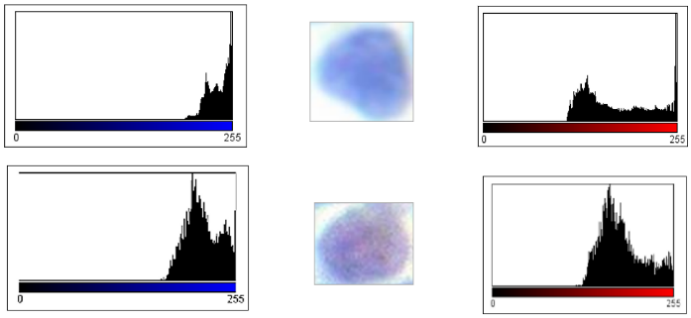

Figure 8: Histogram of overlapping nuclei.

Tests performed on 25 single cells, taken from different samples and labelled differently, revealed that the mitotic cells defined in the blue channel and red channel are delimited in the histogram between 100 and 255 (tint levels) and between 0 and 80 respectively. These cells are marked and calculated without using pixel correction (Figure 3).

Mitotic cells, defined in blue and red histograms between 100 and 255, present overlapping labelling. The mucus

(extracellular substance) is the cause of this color overlap. Our ACCPRO_IMMUNO algorithm acts simultaneously on the spectrum of proliferating cells and mitotic cells. It uses the corrective function CF(r) to solve the overlap problem (Figure 9) (Equation 3).

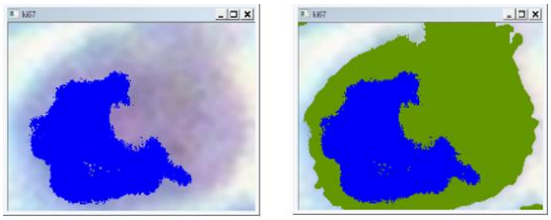

Figure 9: Marking of overlapping nuclei.

$$\forall r \in R,\ \boldsymbol{CF}(r) = \boldsymbol{Pam} = \sum Pdet - \sum Pov \quad (3)$$

CF: Cell Filtering; Pam: Pixels in Active Mitosis, (Active Mitosis); Pov: Overlapping Pixels (Pixel of Overlap); Pdet: Pixel Detected within the Spectrum

ACCPRO_IMMUNO Algorithm calibration

Four sub-images were defined as the number of images needed to average a typical tumour sample for 20 samples stained for Ki-67 by IHC. They have been selected for calibration. First, the visual evaluation of the percentage of positively colored nuclei was distributed from 0% to 100%. Learning slides are visually analyzed by counting positively and negatively colored cells. The proliferation index ki-67 was calculated by the number of stained nuclei DAB divided by the total nuclei. Consequently, samples are analyzed with non-calibrated ACCPRO_IMMUNO and results are compared with visual counting.

The ACCPRO_IMMUNO algorithm is consolidated by the correction function CF(r) (cell filtering). Hence, the obtained results are characterized by good conformity of analysis. These results were used as a standard for calibration of the ACCPRO_IMMUNO algorithm.

Developed software

In order to be widely accepted and used by pathologists, a digital image analysis system must be easy for use and compatible with existing microscopes configurations. For this reason, ACCPRO_IMMUNO application is compatible with Windows operating systems. Moreover, it does not require specific pre-knowledge from the pathologist.

The application allows to:

- Segment the colored DAB/Haematoxylin cells of the image introduced by the user.
- Calculate the percentage of the DAB nuclear zone tinted on the total nuclear surface.
- Reproduce a pseudo-color result image corresponding to the segmentation of two zones.

RESULTS

Figure 10 represents three Ki-67 proliferation levels extracted from the set of images processed by the ACCPRO-UMMINO algorithm.

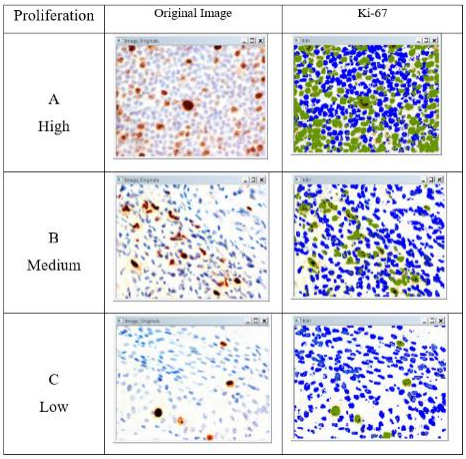

Figure 10: Result Examples of Ki-67-Stained images.

To validate our method, we used 96 samples of Ki-67, chosen randomly. Developed method was implemented in C++ language on a PC with a 2.8 GHz I7 processor, 8 GB of physical RAM and 32 GB of virtual RAM (paging file). Generally, 1 second is needed for the algorithm to process an RGB image of 2040 × 1536 pixels. This meets real-time requirements for clinical use. Good separation of DAB from haematoxylin-stained pixels was obtained, with a 95% pass classification. Therefore, the real-time use and

adaptability of this algorithm to diagnose Ki-67 images help to avoid subjective clinical errors.

Table 1 represents the comparison between the 3 observers and the soft results.

	Obs01	Obs02	Obs03	Algorithm
A	60%	65%	55%	57%
B	20%	25%	23%	26%
C	3%	5%	4%	7%

Table 1: Comparison between observers and algorithm results.

Calibration of ACCPRO_IMMUNO algorithm for the Ki-67 index can be considered as quality assurance factor. The efficiency of the algorithm to the variations of the image preparation and acquisition parameters was examined by comparing the results of several optical resolutions. The used JPEG file format in the acquisition is decompressed without loss of image quality. Additionally, the algorithm is calibrated beforehand according to the actual conditions of preparation.

Evaluation of Luminosity and Contrast Robustness

By varying the contrast and brightness, the algorithm provides robust processing and accurate results. The ratio Ki-67 keeps almost the same value with a variation in contrast of (+ 80% / -80%) (Figure 11) and a variation in brightness (+ 80% / -80%) (Figure 12).

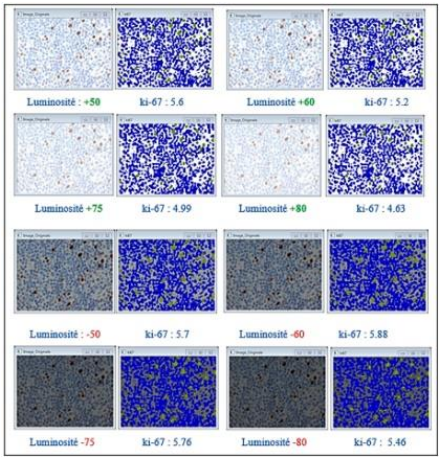

Figure 11: Contrast robustness (+80%/-80%).

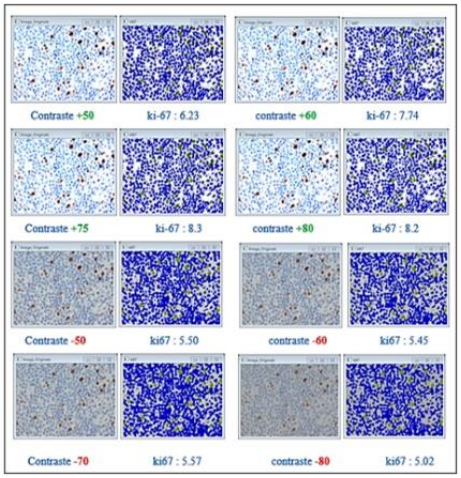

Figure 12: Robustness at brightness (+80%/-80%).

The aforementioned comparison recommends the requirement for pathologists to produce standard images.

Statistic Study

To evaluate statistical significance of obtained results, we calculated confidence interval to define the margin of error for a population of 96 samples. We considered the average of 3 observations from 3 pathologists and the software result. The confidence interval allowed confirming the accuracy of the ACCPRO_IMMUNO automated analysis method. The statistical study was carried out using SPSS software version 17.0.

We used the t-student statistical tool to compare the means of two measurement groups to confirm whether they are statistically significantly different. Two independent groups of measurement were considered for comparison. We used the unpaired t-student test to compare an average of 3 observations with software series. For $\rho = 0.1317$, the difference between the two series of measurements was insignificant. Therefore, we can consider that our automated quantitative proliferation method ACCPRO_IMMUNO is accurate and reliable with a confidence coefficient of 95%.

DISCUSSION

Chemosensitivity depends on the growth rate of cancer cells and drug treatments. Clinical treatment attempts to

give the drug dose that generates the best possible response without causing serious side effects. If the dose is too low, it can affect cancer cells. However, it will not treat cancer effectively. Ki-67 is a continuous index considered as biologically and clinically relevant cut point as confirmed by meta-analyses (15,000 patients) [27]. Therefore, acting on the accuracy of this index is an important factor for the pathologist to refine the diagnosis. It allows the clinician to choose the optimal treatment for his patients.

In this line of research, manual evaluation can, in certain cases, leads to significant inter-observer results variability [28]. Moreover, in an inter-laboratory study of 172 pathologists, 24% of positive slides were translated as false-negative [19]. Therefore, the cause of this deviation is the contingent quality of the images (noise, color overlap on cores, contrast and brightness). Hence, to overcome most of these difficulties and guarantee more precise results (PER: Proliferation Evaluate Rate), we emphasize that a clear marked slide ensures better separation of the DAB/Haematoxylin nuclei at the manual and algorithmic analysis level.

CONCLUSION

In this study, the estimation PRE in BC was performed by the Ki-67 prognostic markers and the development of an accurate user-friendly automated tool for histochemical image processing. Objective measurements were based on an adequate pre-treatment of acquired images as well as a precise spectro colorimeter treatment of the histochemical images. The developed ACCPRO_IMMUNO software can be an important future tool for the improvement, the precision and the reproducibility of Ki-67 tests. In addition, it will be of great interest in reducing inter-observer results variability in the fields of diagnosis and research.

CONFLICT OF INTEREST

The authors have no conflicts of interest to declare.

REFERENCES

1. EL-Adalany MA, EL-Razek AAEKA, EL-Metwally D (2021) Prediction of nipple-areolar complex involvement by breast cancer: Role of dynamic contrast-enhanced magnetic resonance imaging (DCE-MRI). Egyptian Journal of Radiology and Nuclear Medicine 52(1): 1-8.
2. Zhang QW, Gao YJ, Zhang RY, et al. (2020) Personalized CT-based radiomics nomogram preoperative predicting Ki-67 expression in gastrointestinal stromal tumors: A multicenter development and validation cohort. Clinical and Translational Medicine 9(1): 1-11.
3. Rexhepaj E, Brennan DJ, Holloway P, et al. (2008) Novel image analysis approach for quantifying expression of nuclear proteins assessed by immunohistochemistry: Application to measurement of oestrogen and progesterone receptor levels in breast cancer. Breast Cancer Research 10(5): 1-10.
4. Zaha DC (2014) Significance of immunohistochemistry in breast cancer. World Journal of Clinical Oncology 5(3): 382.
5. Rahmanzadeh R, Huttmann G, Gerdes J, et al. (2007) Chromophore-assisted light inactivation of pKi-67 leads to inhibition of ribosomal RNA synthesis. Cell Proliferation 40(3): 422-430.
6. Beresford MJ, Wilson GD, Makris A (2006) Measuring proliferation in breast cancer: Practicalities and applications. Breast Cancer Research 8(6): 1-11.
7. Shi P, Zhong J, Hong J, et al. (2016) Automated Ki-67 quantification of immunohistochemical staining image of human nasopharyngeal carcinoma xenografts. Scientific Reports 6(1): 1-9.
8. Saha M, Chakraborty C, Arun I, et al. (2017) An advanced deep learning approach for Ki-67 stained hotspot detection and proliferation rate scoring for prognostic evaluation of breast cancer. Scientific Reports 7(1): 1-14.

9. Swiderska Z, Korzynska A, Markiewicz T, et al. (2015) Comparison of the manual, semiautomatic, and automatic selection and leveling of hot spots in whole slide images for Ki-67 quantification in meningiomas. Analytical Cellular Pathology 2015: 498746.
10. Fiore C, Bailey D, Conlon N, et al. (2012) Utility of multispectral imaging in automated quantitative scoring of immunohistochemistry. Journal of Clinical Pathology 65(6): 496-502.
11. Kearney SJ, Black JC, Landis BJ, et al. (2017) Analytical validation of Ki67/CD8 duplex IHC assay using computational tissue analysis (cTATM). Cancer Research 77(13_Supplement): 763-763.
12. Tuominen VJ, Ruotoistenmäki S, Viitanen A, et al. (2010) ImmunoRatio: A publicly available web application for quantitative image analysis of estrogen receptor (ER), progesterone receptor (PR), and Ki-67. Breast Cancer Research 12(4): 1-12.
13. Allred DC, Carlson RW, Berry DA, et al. (2009) NCCN task force report: Estrogen receptor and progesterone receptor testing in breast cancer by immunohistochemistry. Journal of the National Comprehensive Cancer Network 7(Suppl_6): S-1.
14. Leal S, Diniz C, Sá C, et al. (2006) Semiautomated computer-assisted image analysis to quantify 3, 3′-diaminobenzidine tetrahydrochloride-immunostained small tissues. Analytical Biochemistry 357(1): 137-143.
15. Ruifrok AC, Johnston DA (2001) Quantification of histochemical staining by color deconvolution. Analytical and Quantitative Cytology and Histology 23(4): 291-299.
16. Pham NA, Morrison A, Schwock J, et al. (2007) Quantitative image analysis of immunohistochemical stains using a CMYK color model. Diagnostic pathology 2(1): 1-10.
17. Ruifrok AC, Katz RL, Johnston DA (2003) Comparison of quantification of histochemical staining by hue-saturation-intensity (HSI) transformation and color-deconvolution. Applied Immunohistochemistry & Molecular Morphology 11(1): 85-91.
18. Xing F, Su H, Yang L (2013) An integrated framework for automatic Ki-67 scoring in pancreatic neuroendocrine tumor. In International Conference on Medical Image Computing and Computer-Assisted Intervention: 436-443.
19. Rüdiger T, Höfler H, Kreipe HH, et al. (2002) Quality assurance in immunohistochemistry: Results of an interlaboratory trial involving 172 pathologists. The American Journal of Surgical Pathology 26(7): 873-882.
20. Walker RA (2006) Quantification of immunohistochemistry-issues concerning methods, utility and semiquantitative assessment I. Histopathology 49(4): 406-410.
21. Taylor CR, Levenson RM (2006) Quantification of immunohistochemistry-issues concerning methods, utility and semiquantitative assessment II. Histopathology 49(4): 411-424.
22. Romero Q, Bendahl PO, Fernö M, et al. (2014) A novel model for Ki67 assessment in breast cancer. Diagnostic pathology 9(1): 1-8.
23. Rojo MG, Bueno G, Slodkowska J (2009) Review of imaging solutions for integrated quantitative immunohistochemistry in the Pathology daily practice. Folia Histochemica et Cytobiologica 47(3): 349-354.
24. Fu R, Ma X, Bian Z, et al. (2015) Digital separation of diaminobenzidine-stained tissues via an automatic color-filtering for immunohistochemical quantification. Biomedical Optics Express 6(2): 544-558.
25. Brey EM, Lalani Z, Johnston C, et al. (2003) Automated selection of DAB-labeled tissue for immunohistochemical quantification. Journal of Histochemistry & Cytochemistry 51(5): 575-584.
26. Stuart-Harris R, Caldas C, Pinder SE, et al. (2008) Proliferation markers and survival in early breast cancer: A systematic review and meta-analysis of 85 studies in 32,825 patients. The Breast 17(4): 323-334.
27. Rojo MG, Bueno G, Slodkowska J (2009) Review of imaging solutions for integrated quantitative immunohistochemistry in the Pathology daily practice. Folia Histochemica et Cytobiologica 47(3): 349-354.
28. Klauschen F, Wienert S, Schmitt WD, et al. (2015) Standardized Ki67 diagnostics using automated scoring-clinical validation in the gepartrio breast cancer study clinically validated automated Ki67 scoring. Clinical Cancer Research 21(16): 3651-3657.